Growth and characterization of doped GaAs/AlGaAs multiple quantum well structures on Si substrates for infrared detection

Y. J. Mii, R. P. G. Karunasiri, and K. L. Wang
Device Research Laboratory, Department of Electrical Engineering, University of California, Los Angeles, California 90024

Gang Bai
California Institute of Technology, Pasadena, California 91125

(Received 22 September 1988; accepted 22 September 1988)

Doped GaAs/AlGaAs multiple quantum well structures were grown on Si substrates by molecular-beam epitaxy. The crystallinity of the epitaxial layers was examined by cross-sectional transmission electron microscopy and an x-ray rocking curve technique. The threading dislocation density of the multiple quantum well region was estimated to be 10^8 cm^{-2} by transmission electron microscopy. The x-ray rocking curve measurement revealed a full width at half-maximum of 380 arcsec, with no superlattice peak observed. Electrical and optical characterizations by tunneling current and intersubband infrared absorption showed comparable properties with similar structures grown directly on a GaAs substrate. The effect of crystallinity on the electrical and optical properties of the multiple quantum well structures is discussed.

I. INTRODUCTION

GaAs on Si technology has drawn a great deal of interest in recent years, because of its potential application of optoelectronic integration circuit (OEIC).[1] However, the high density of threading dislocations and thermal stress in the GaAs on Si epitaxial layer severely degrades the performance of most electro-optic devices such as lasers[2,3] and light emitting diodes (LED's).[4] During the past few years, a new type of electro-optic device using a doped GaAs/AlGaAs multiple quantum well (MQW) for long wavelength (near 10 μm) infrared (IR) detection were studied both experimentally[5–10] and theoretically.[11,12] Novel infrared detectors based on this MQW structure were successfully demonstrated[10] with responsivity and detectivity comparable to that of HgCdTe devices. Since the operation of this type of device is based on majority carriers, it should be less sensitive to threading dislocations and more suitable for integration with Si circuits. Combined with the current GaAs on Si technology, it may facilitate a new class of OEIC for IR imaging application. A recent demonstration of double barrier resonant tunneling diodes on Si substrate with high peak-to-valley current ratio[13] also supports this suggestion. In this study, the growth and characterization of the doped GaAs/AlGaAs MQW on Si substrates by molecular-beam epitaxy (MBE) will be described.

II. EXPERIMENT

The samples were grown by a computer-controlled Perkin–Elmer 430 MBE system. To avoid the formation of antiphase domains and to reduce the threading dislocation density, Si substrates oriented at [100] tilted 3° toward [011] were used for MBE growth of GaAs.[1] High resistivity p-type Si wafers were used in this experiment to reduce the free-carrier IR absorption. The Si substrates were cleaned by the Shiraki method[14] and the protective thin oxide layers on the Si substrates were desorbed at 830 °C under incidence of a Ga flux[15] for 20 min. The GaAs layers were grown by a two-step growth technique.[1] First, an 800-Å-thick initial layer was grown at 400 °C with a 0.4 μm/h growth rate, then the substrate temperature and growth rate were increased to 600 °C and 1 μm/h, respectively. A 1.7-μm-thick GaAs buffer layer was grown after deposition of the initial layer to reduce the threading dislocation density of the active region to 10^8 cm^{-2}. The top 1-μm buffer layer was doped with Si to 3×10^{18} cm^{-3} for making Ohmic contacts in the tunneling current measurement experiment. The MQW structures consist of 50 GaAs wells of 65 Å thickness sandwiched between 95-Å undoped $Al_xGa_{1-x}As$ barriers. Only the center 50 Å of the wells was doped with Si to 1.5×10^{18} cm^{-3}. A 0.5-μm GaAs cap layer was grown on top of the MQW with a doping concentration of 3×10^{18} cm^{-3}. Two samples with 25% and 30% Al concentrations in $Al_xGa_{1-x}As$ barriers were grown for this study. Also, another sample was grown without the MQW as the reference for IR absorption measurement.

The 30% Al sample was prepared for cross-sectional transmission electron microscopy (TEM) and x-ray rocking curve measurements. The IR absorption spectra were measured at room temperature using a Fourier transform infrared spectrometer (FTIR). The samples were mounted at Brewster's angle (73°) to the incident IR beam. A FTIR measurement using a multiple-pass waveguide geometry was also performed for the 30% Al sample. To measure tunneling currents, a AuGe/Ni/Au alloy was used for ohmic contacts. Mesa diodes with diameters from 25 to 100 μm were fabricated from both samples.

III. RESULTS AND DISCUSSION

Figure 1 shows the cross-sectional TEM of the 30% Al sample. The threading dislocation density at the MQW region was $\sim10^8$ cm^3. The average spacing between dislocations is ~1 μm. Comparing with the electron mean free path at 77 K, which is estimated to be <900 Å (Refs. 16, 17) for the doped well (10^{17} to 10^{18} cm^{-3}), the effect of dislocations

 0734-211X/89/020341-04$01.00

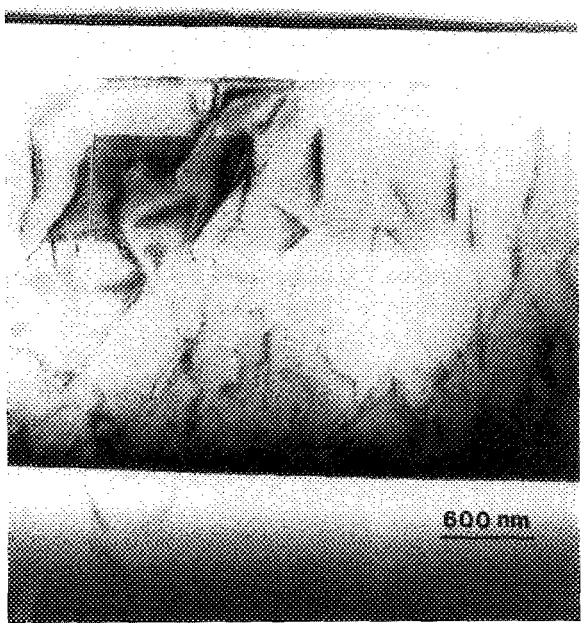

FIG. 1. Cross-sectional TEM of the 30% Al MQW grown on Si. The threading dislocation density at the MQW region is $\sim 10^8$ cm^{-2}.

on electron scattering can be neglected. However, for modulation doped MQW's, the low-temperature mobility value can exceed 100,000 cmV^{-1} s^{-1},[16] and the electron mean free path becomes larger than 1 μm. In this case, the scattering by dislocations should not be ignored. The MQW structure, examined by TEM, is shown in Fig. 2. Fairly smooth and uniform GaAs and AlGaAs layers with some surface waviness of < 70 Å/μm was observed. The total thickness of the MQW was determined to be ~ 7000 Å. Based on the TEM data, the actual well and barrier width should be 60 and 85 Å, respectively. The observed x-ray rocking curve data and numerical simulation results are shown in Fig. 3. The x-ray

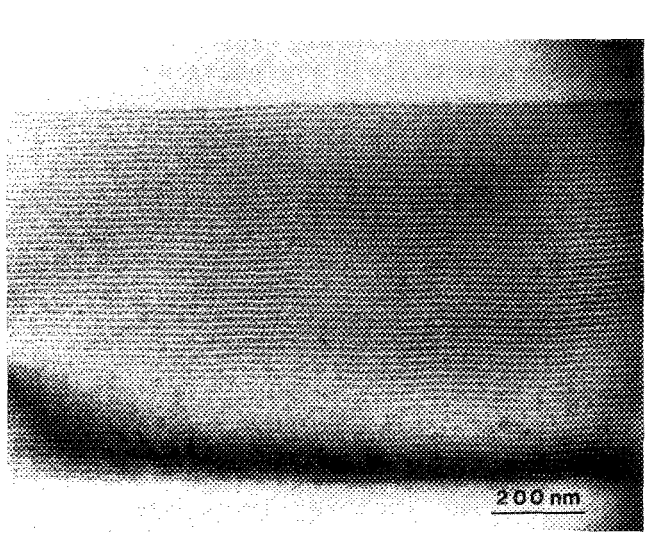

FIG. 2. A closer look of the MQW structure by TEM. The total thickness of MQW measured from TEM picture is ~ 7000 Å.

rocking curve of the same sample shows a full width at half-maximum (FWHM) of 380 arcsec, larger than our normal GaAs/Si sample (~ 300 arcsesc). Due to the broadening of the GaAs peak by the high threading dislocation density, the superlattice peaks were not observable in our experiment.

Figure 4 shows the absorption spectra for both samples measured at room temperature. For the sample with 25% Al, the absorption peak appeared at 1100 cm^{-1} (136 meV) and has a FWHM of 175 cm^{-1}. For the sample with 30% Al, the absorption peak appears at a shorter wavelength of 1240 cm^{-1} (154 meV), and has a FWHM of 190 cm^{-1}. The peak shift toward a shorter wavelength is due to the increase of the energy level separation in the quantum well when the barrier height of this sample is increased. For similar MQW's grown on GaAs substrates, the absorption peak linewidths of 100–170 cm^{-1} (Refs. 6,7) had been reported. The IR transmission spectrum measured in the multiple-pass waveguide geometry of the 30% Al sample is also depicted in Fig. 5. Almost 100% absorption was observed near the peak position. However, this strong absorption, which saturated our FTIR measurement, obscured the determination of the exact peak position.

The bound-state energies of the quantum well were calculated by using an envelope function approximation and taking into account the finite barrier heights and the different effective masses in the barrier and the well. Using the quantum well thickness of 60 Å, the calculated energy separation of the first two levels for the 25% Al sample is 127 meV and for the 30% Al sample is 149 meV. These energies agree well with the experimental observed values.

From the absorption spectra, the oscillator strength for the transition between the ground and the first excited states are estimated to be 15 and 11 for the 25% and 30% Al samples,[18] respectively. For similar structures grown on a GaAs substrate, an oscillator strength of typically 8–17 was observed.[6–9]

At room temperature, the current–voltage (I–V) characteristic shows no apparent features. When cooled down to low temperature, negative differential conductance emerges. The I–V characteristics measured at 77 K for both the 25% and 30% Al samples are shown in Fig. 6. The multiple negative conductance by sequential resonant tunneling can be better examined by the conductance–voltage (G–V) curve as depicted in Fig. 7. A detailed discussion of the tunneling current measurement has been described elsewhere.[18] By using the first negative differential conductance peaks, occurring at 0.53 ± 0.1 V and 0.68 ± 0.08 V for the 25% and 30% Al samples, respectively, the ground-state broadening can be estimated to be 10 meV, and the scattering time is obtained to be $\tau = 7 \times 10^{-14}$ s. For similar structures grown on GaAs substrates, a 7-meV ground-state broadening and $\tau = 1 \times 10^{-13}$ s were obtained. The effect of dislocations on electron scattering in the doped wells is small as discussed before.

The low bias I–V curves, which are approximately linear, can be evaluated by the ground-state sequential tunneling,[8]

$$I = \frac{eA}{\hbar L^2} D_0 kT \ln\left[\frac{1 + e^{E_f/kT}}{1 + e^{(E_f - eV)/kT}}\right] \quad (2)$$

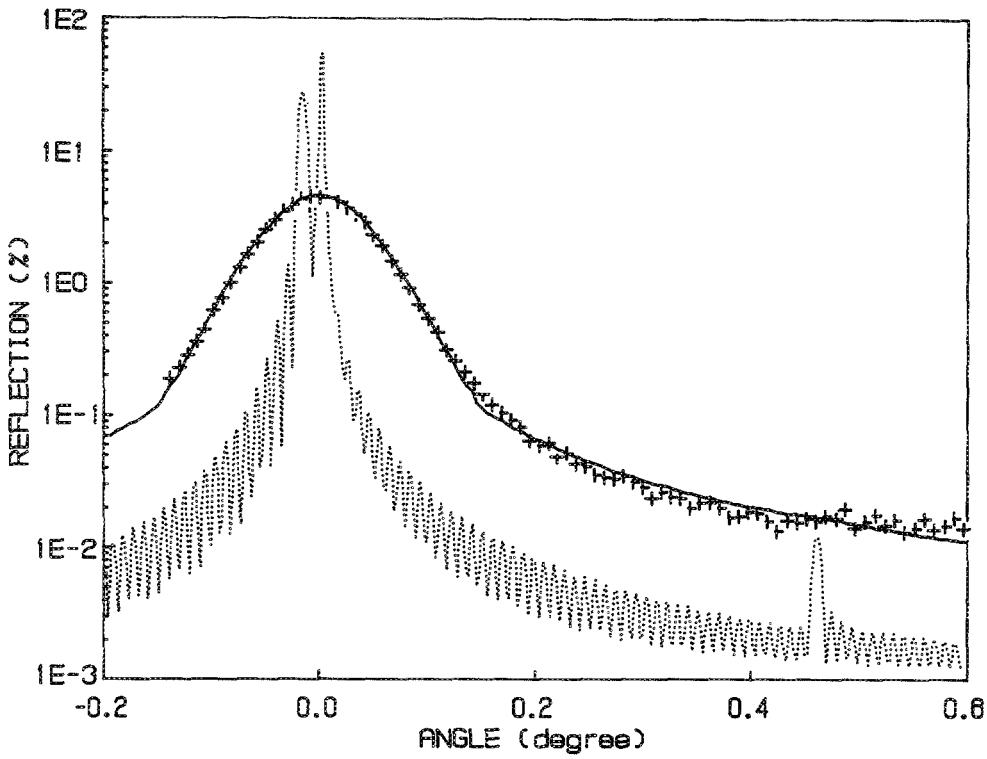

FIG. 3. X-ray rocking curve data and simulation results. The crosses are the measured x-ray rocking curve data. The dotted line is the ideal reflection from the 160-Å period GaAs/AlGaAs MQW. The solid line is the convolution of the ideal curve with broadening, which fits the measured data. The superlattice peaks are not observable in this experiment.

where D_0 is the tunneling coefficient of the individual barriers, A is the area of the device, L is the well thickness and E_f is the Fermi level. The tunneling coefficient D_0 can be obtained by the WKB approximation,[8]

$$D_0 = \exp\left[\frac{-4L_b}{3eV\hbar}(2m_b^*)^{1/2} \times [(H-E_1)^{3/2} - (H-E_1-eV)^{3/2}]\right]. \quad (3)$$

In this equation, L_b is the barrier width, H is the barrier height, V is the average voltage drop per period and m_b^* is the effective mass of the barrier. Using the 60% band discontinuity rule and band gap data by Casey and Panish[19] as well as the TEM calibrated values of $L_b = 85$ Å and $L_w = 60$ Å, the low bias current of the 30% Al sample can fit within 20% of the experimental data. For the 25% Al sample, however, $L_b = 90$ Å and $L = 60$ Å fit better with the I–V curve.

IV. CONCLUSION

Intersubband IR absorption and sequential resonant tunneling are clearly observed in doped GaAs/AlGaAs MQW structures grown on a Si substrate. The electrical and optical properties of the MQW's on Si are comparable to similar structures grown directly on a GaAs substrate, and fit very

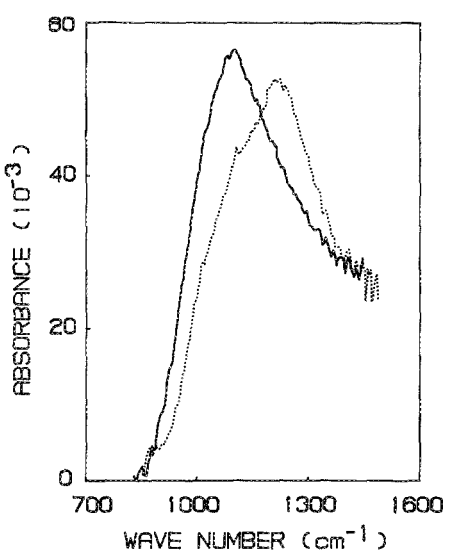

FIG. 4. Measured IR absorbance of 25% (solid line) and 30% (dotted line) Al samples. The absorption peak of the 25% Al sample appeared at 9.1 μm and the absorption peak of the 30% Al sample appeared at 8.1 μm.

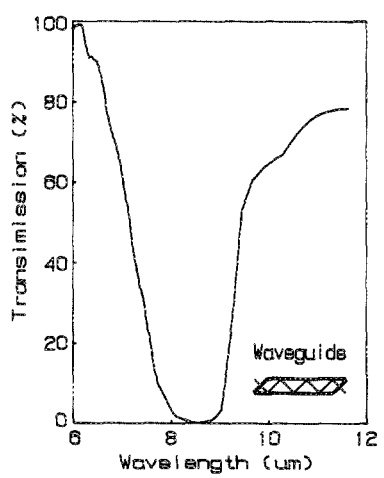

FIG. 5. IR transmission spectrum measured in the multiple-pass waveguide geometry of the 30% Al sample. Absorption is strongly enhanced due to the multiple pass and is almost 100% near the peak. The absorption peak position is difficult to determine because of the strong absorption, which saturated the FTIR measurement.

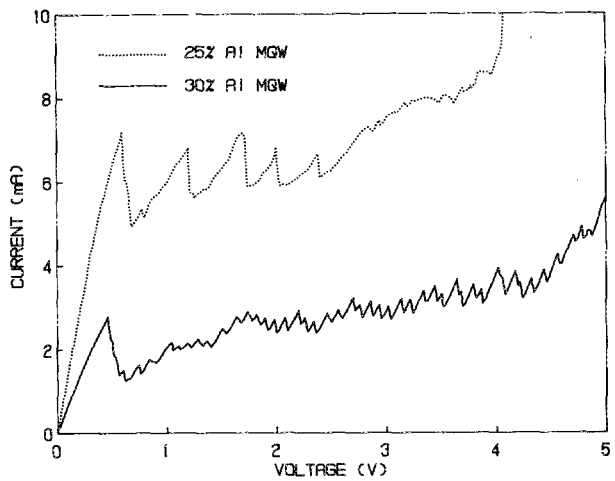

FIG. 6. Current–voltage characteristics with sequential resonant tunneling of 25% and 30% Al samples measured at 77 K. The diameter of mesa diodes is 50 μm.

well with theoretical calculations. Threading dislocations and waviness seem to have little effect on the MQW structures with doped wells. This may not be true for the modulation doped MQW structures as discussed previously. The devices are stable during thermal cycling between 77 to 300 K, and no degradation is observed during the experimental period. The new majority carrier type electro-optic devices using doped MQW's appear to be suitable for integration with Si very large scale integrated circuits from this preliminary observation. Investigations of photoresponsivity and detectivity measurement should provide further information about device performance.

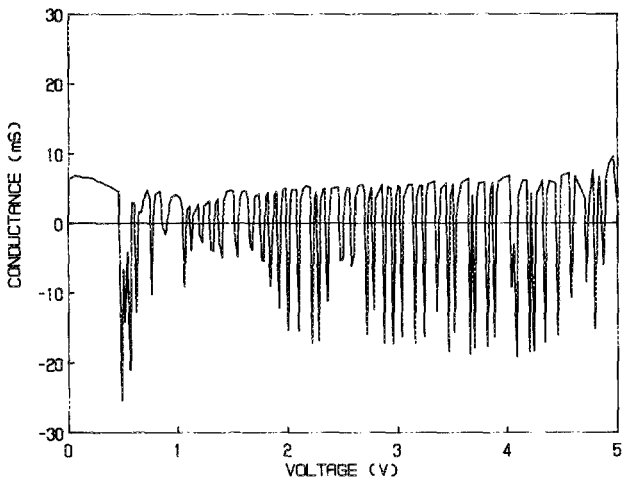

FIG. 7. Conductance–voltage curves of the 30% Al sample derived from Fig. 6. Multiple negative differential conductance peaks by sequential resonant tunneling are observed.

ACKNOWLEDGMENTS

The authors would like to thank Dr. R. Alt at Aerospace Corporation for FTIR measurements. This work was supported in part by DOD-URIP under ONR and ARO and by Intel-Micro program.

[1] J. S. Harris, Jr., S. M. Koch, and S. J. Rosner, *Heteroepitaxy on Silicon*, edited by J. C. C. Fan, J. M. Philips, and B. Tsau (MRS, Pittsburgh, 1987), p. 3.
[2] T. H. Windhorn, G. W. Turner, and G. M. Metze, in Ref. 1, p. 157.
[3] H. Z. Chen, A. Ghaffari, H. Wang, H. Morkoç, and A. Yariv, Appl. Phys. Lett. **51**, 1320 (1987).
[4] H. K. Choi, G. W. Turner, T. H. Windhorn, and B. Tsau, IEEE Electron Dev. Letts. **7**, 500 (1986).
[5] J. S. Smith, L. C. Chiu, S. Margalit, A. Yariv, and A. Y. Cho, J. Vac. Sci. Technol. B **1**, 376 (1983).
[6] L. C. West and S. J. Eglash, Appl. Phys. Lett. **46**, 1156 (1985).
[7] B. F. Levine, K. K. Choi, C. G. Bethea, J. Walker, and R. J. Malik, Appl. Phys. Lett. **50**, 1092 (1987).
[8] K. K. Choi, B. F. Levine, R. J. Malik, J. Walker, and C. G. Bethea, Phys. Rev B **35**, 4172 (1987).
[9] A. Harwit and J. S. Harris, Jr., Appl. Phys. Lett. **50**, 685 (1987).
[10] B. F. Levine, C. G. Bethea, G. Hasnain, J. Walk, and R. J. Malik, Appl. Phys. Lett. **53**, 296 (1988).
[11] D. D. Coon and R. P. G. Karunasiri, Appl. Phys. Lett. **45**, 649 (1984).
[12] K. W. Goossen and S. A. Lyon, Appl. Phys. Lett. **47**, 1257 (1985).
[13] S. C. Kan, H. Morkoç, and A. Yariv, Appl. Phys. Lett. **52**, 2250 (1988).
[14] A. Ishizaka, K. Nakagawa and Y. Shiraki, in *Proceedings of the 2nd International Symposium on Molecular Beam Epitaxy and Related Clean Surface Techniques* (Japanese Society of Applied Physics, Tokyo, 1982), p. 183.
[15] S. Wright and H. Kroemer, Appl. Phys. Lett. **36**, 210 (1980).
[16] H. Morkoç, *The Technology and Physics of Molecular Beam Epitaxy*, edited by E. H. C. Parker (Plenum, New York, 1985), p. 185.
[17] R. A. Smith, *Semiconductors* (Cambridge, Cambridge, 1978), p. 101.
[18] Y. J. Mii, R. P. G. Karunasiri, and K. L. Wang, Appl. Phys. Lett. **53**, 2050 (1988).
[19] H. C. Casey, Jr., and M. B. Panish, *Heterostructure Lasers*, Part A and B (Academic, New York, 1978).